Journal of Chromatography A, 1218 (2011) 5423–5433

Contents lists available at ScienceDirect

Journal of Chromatography A

journal homepage: www.elsevier.com/locate/chroma

Multiple-injection technique for isolating a target protein from multicomponent mixtures☆

Wojciech Marek, Wojciech Piątkowski, Dorota Antos*

Chemical and Process Engineering Department, Rzeszow University of Technology, W. Pola Str., 2, 35-959 Rzeszow, Poland

ARTICLE INFO

Article history:
Received 9 November 2010
Received in revised form 14 February 2011
Accepted 15 February 2011
Available online 22 February 2011

Keywords:
HIC
IEC
Injection technique
Process integration
Sample-solvent

ABSTRACT

An integrated chromatographic process comprising ion exchange (IEC) and hydrophobic interaction chromatography (HIC) for isolating a target protein form multicomponent mixtures has been analyzed. The model mixture contained immunoglobulin G that was the key product of the separation process, cytochrome C and ovalbumin. The adsorption characteristics and the mass transport kinetics of the model proteins have been determined along with their dependencies on the operating variables such as pH, temperature and the salt concentration for IEC as well as HIC media. Limitations of the process efficiency resulting from kinetic effects, solubility constraints and the necessity of the mobile phase exchange between chromatographic steps have been discussed. To improve the performance of the integrated process the multiple-injection technique has been suggested. This technique consisted in loading feed mixtures dissolved in a good solvent onto the column by several small-volume injections under conditions of strong protein adsorption. It allowed diminishing interactions between the sample-solvent and protein and elimination of undesired effects such as band splitting and band broadening. For the process design and optimization a dynamic model has been used accounting for thermodynamics and kinetics of the process. The optimization results indicated superiority of the multiple-injection technique over standard isocratic injections in terms of the process yield and productivity.

1. Introduction

Nowadays large demand for proteins is recognized, particularly by pharmaceutical industry and biotechnology. The increasing regulatory requirements enforce the necessity of manufacturing high-purity proteins; therefore, downstream processing is a critical step of the overall production process.

Purification of macromolecules may comprise several high-resolution separation stages (two, three, four or more) and in many cases final polishing when product is used for therapeutical applications. Chromatography as a highly selective separation method is often a key operation in the downstream processing. To isolate a target protein from complex multicomponent mixtures a combination of different chromatographic techniques have to be employed. Usually few chromatographic stages differing in the separation mechanism are necessary to achieve desired selectivity of the separation [1–3].

Integration of different chromatographic techniques requires determining and synchronizing a number of operating parameters such as the mobile phase composition, pH and temperature to ensure high efficiency of the whole operation. Each of chromatographic techniques utilizes different type and composition of buffered mobile phases; therefore, additional step of buffer exchange between the stages is necessary. Moreover, chromatographic elution of proteins is accompanied by strong dilution of feed mixtures originating from kinetic effects. Thus, transferring mixtures to be separated between subsequent chromatographic stages requires additional operation of protein concentration. Another performance limitation is the solubility constraint. Solubility of proteins strongly depends on pH, type and concentration of salt in solutions used as the mobile phase [1].

To overcome those limits different solvents can be used to inject protein mixtures and to elute them. The choice of the solvent for the feed stream depends on the sequence of chromatographic stages, solubility constraints and separation selectivity. However, such an injection methodology may cause undesired effects, such as band splitting and band deformations [4–16]. In our previous study these phenomena were analyzed in hydrophobic interaction chromatography [16]. It was shown that proper selection of the operating conditions for the sample injection allowed increase of the mass loadings while undesirable effects of band deformations could be avoided. The method was indicated to be suitable for increasing the loading concentration; however, it forced a restriction on the loading volume.

In this study that idea was extended to increase both the concentration and volume loading. The multiple-injection technique

☆ Presented at the 13th Symposium on Preparative and Industrial Chromatography and Allied Techniques, Stockholm, Sweden, 12–15 September 2010.

* Corresponding author. Tel.: +48 17 865 1730.
E-mail address: ichda@prz.rzeszow.pl (D. Antos).

0021-9673/$ – see front matter © 2011 Elsevier B.V. All rights reserved.
doi:10.1016/j.chroma.2011.02.039

Nomenclature

c	concentration in the mobile phase
D_L	axial dispersion coefficient
F	phase ratio, $(1-\varepsilon_t)/\varepsilon_t$
k	kinetic coefficient
K	equilibrium constant
L	column length
N	number of theoretical plates
Pr	productivity
Pu	purity
q	concentration in the adsorbed phase
x	space coordinate
t	time coordinate
t,T	temperature, in proper scale
u	superficial velocity
$\dot{V}$	flowrate
w	interstitial velocity
Y	yield

Greek symbols

ε_t, ε_e	total and external bed porosity, respectively

Subscripts and superscripts

a	denotes adsorption
d	denotes desorption
f	denotes folding
F	denotes feed
in	denotes inlet
inj	denotes injection
n	denotes native form
p	denotes protein
salt	denotes salt
sol	denotes solubility
unf	denotes unfolding
wash	denotes washing
0	denotes initial conditions

was exploited to overcome performance limitations of chromatographic elution and to integrate different chromatographic techniques. The integrated process comprised two chromatographic stages typically used in an industrial scale: ion exchange chromatography (IEC) and hydrophobic interaction chromatography (HIC).

The mechanism of IEC separation is based on electrostatic interactions between the protein and charged column matrix. The proteins are separated according to the nature and degree of their ionic charge. Elution is effected by increasing the ionic strength and, thus, concentration of salt containing counter ions that compete with the protein molecules for the charged active centers on the matrix [1,2]. Because of the nature of the separating mechanism, pH plays important roles in controlling the separation.

HIC is often employed as an alternative or supplementary technique to IEC [17,18]. It exploits the interaction between hydrophobic surface sites of both native proteins and column matrix, requiring consequently strong salting-out solvents for binding [19]. Protein adsorption is induced by high concentration of structure-enhancing salts (cosmotrope) such those used in precipitation (e.g. ammonium sulphate) and followed by elution with a descending salt concentration. The retention properties of proteins in HIC are strongly altered by temperature. In general, increasing temperature enhances hydrophobic interactions and the protein retention whereas lowering temperature promotes the protein elution [17,20–22].

It is evident that both these techniques utilize different operating conditions; hence, their proper integration is of major importance for the purification performance.

In this study HIC and IEC were integrated to isolate a target protein from a ternary mixture. For the process design a lumped dynamic model was used accounting for underlying kinetics, i.e., rates of adsorption–desorption and conformational changes. Relevant kinetic dependencies indispensable to the process design were experimentally quantified and incorporated into the model.

2. Theory

2.1. Mathematical modeling

To simulate band profiles the kinetic-dispersive model was employed. It consists of the mass balance equation of the component i in the mobile phase:

$$\varepsilon_t \frac{\partial c_i}{\partial t} + u\frac{\partial c_i}{\partial x} + (1-\varepsilon_t)\frac{\partial q_i}{\partial t} = \varepsilon_e D_{L,i}\frac{\partial^2 c_i}{\partial x^2} \tag{1}$$

where c_i is the concentration of species in the mobile phase; $i = p$ (*protein*) or *salt*; u is the superficial velocity, t, x are time and axial coordinates, D_L is the axial dispersion coefficient, q_i is the adsorbed phase concentration, ε_t, ε_e are the total and external bed porosity, respectively.

For the Langmuir type of adsorption behavior Eq. (1) can be combined with the following kinetic equation:

$$\frac{\partial q_i}{\partial t} = k_{d,i}(K_{e,i}c_i(q^\infty - q_i) - q_i) \tag{2}$$

where q^∞ is the saturation capacity, $K_{e,i} = k_{a,i}/k_{d,i}$ is the equilibrium constant, $k_{a,i}$, $k_{d,i}$ are the rate coefficients of adsorption and desorption.

Due to kinetic limitations chromatographic elution of protein is usually accompanied by strong band dilution. In this case $q^\infty >> q_i$ and Eq. (2) simplifies to:

$$\frac{\partial q_i}{\partial t} = k_{d,i}(K_i c_i - q_i) \tag{3}$$

where $K_i = K_{e,i}q^\infty$ is the distribution coefficient, termed also as the Henry constant.

For non-retained salts the value of the distribution coefficient can be set equal to zero $K_{salt} = 0$.

The protein unfolding was assumed to occur in the adsorbed phase according to the reversible reaction mechanism:

$$P \underset{k_d}{\overset{k_a}{\rightleftarrows}} P_n \underset{k_f}{\overset{k_{unf}}{\rightleftarrows}} P_{unf} \tag{4}$$

represented by the following kinetic equations [16,23,24]:

$$\frac{\partial q_n}{\partial t} = k_{d,p}(K_p c_p - q_n) - k_f(K_{unf}q_n - q_{unf}) \tag{5}$$

$$\frac{\partial q_{unf}}{\partial t} = k_f(K_{unf}q_n - q_{unf}) \tag{6}$$

where $K_{unf} = k_{unf}/k_f$ is the unfolding equilibrium constant, k_f and k_{unf} are the folding and unfolding rate coefficients, respectively, q_n, q_{unf} is the concentration of the protein (P) adsorbed on the surface in the native (P_n) and unfolded form (P_{unf}), respectively.

Then, the accumulation term in Eq. (1) can be expressed as:

$$\frac{\partial q_p}{\partial t} = \frac{\partial q_n}{\partial t} + \frac{\partial q_{unf}}{\partial t} \tag{7}$$

The model parameters ($\boldsymbol{k}$) such as the equilibrium constants, K_p, K_{unf} and the kinetic coefficients, $k_{d,p}$, k_f, depend on the salt concentration, temperature and pH:

$$\boldsymbol{k} = f_{\boldsymbol{k}}\,(c_{salt}, T, \mathrm{pH}), \qquad \boldsymbol{k} = K_p, K_{unf}, k_{d,p}, k_f \tag{8}$$

To solve the set of mass balance equations for the solute and salt, initial and boundary conditions should be specified as follows:

- Initial conditions:for $t = 0$

$$c_i(t, x) = c_{i,0} \tag{9}$$

Typically, for the solute $c_{p,0} = 0$

- Boundary conditions:The Danckwerts-type boundary conditions were assumed:for $t > 0$• at the column inlet it holds:$x = 0$

$$u(c_{i,in}(t) - c_i(t, x)) = -\varepsilon_e D_L \frac{\partial c_i(t, x)}{\partial x} \tag{10}$$

where $c_{i,in}(t)$ defines the injection profile.

The function $c_{i,in}(t)$ can be used to describe the inlet profile of the solute as well as of salt.

An injection cycle consists of two stages: the injection step for the input of the solute dissolved in the sample-solvent and the washing step for elution of the sample-solvent. The mobile phase for the washing step (washing-solvent) should be properly selected to promote strong adsorption of protein. In the injection cycle the sample-solvent can be eluted while the target solute has to retain in the column. A single injection cycle is illustrated by the following conditions:

- for the solute p

$$c_{p,in}(t) = \begin{cases} c_{p,F} & \text{for} \quad t \in [0, t_{inj}] \\ 0 & \text{for} \quad (t_{wash} + t_{inj}) > t > t_{inj} \end{cases} \tag{11}$$

where $c_{p,F}$ is the feed concentration, t_{inj} is the width of the pulse (injection time), t_{wash} is the washing time between consecutive injections.

- for the salt

$$c_{salt,in}(t) = \begin{cases} c_{salt,F} & \text{for} \quad t \in [0, t_{inj}] \\ c_{salt,wash} & \text{for}\,(t_{inj} + t_{wash}) > t > t_{inj} \end{cases} \tag{12}$$

where $c_{salt,F}$ is the salt concentration in the feed stream, $c_{salt,wash}$ is the salt concentration in the washing step. The injections can be repeated in n_{cyc} subsequent cycles.

Elution of the solute is performed after the injection cycle under gradient conditions. For a step gradient that consists of n_{grad} steps with the time duration Δt_j starting at time t_j, the function $c_{salt,in}(t)$ can be described as:

$$c_{salt,in}(t) = c_{salt,j} \quad \text{for} \quad t \in [t_j, t_j + \Delta t_j] \quad j = 1, .., n_{grad} \tag{13}$$

- At the column outlet it holds:

$x = L$

$$\frac{\partial c_i(t, x)}{\partial x} = 0 \tag{14}$$

2.2. Optimization of the process performance

A typical objective of separation is to maximize the process productivity defined as mass flowrate of pure target product withdrawn in the outlet of the system:

$$Pr_p = \dot{m}_{product} = \frac{V_{inj} c_{p,F} Y_{p,out}}{\Delta t_d} \tag{15}$$

where $c_{p,F}$ is the feed concentration of the target product p, V_{inj} is the injection volume, Δt_d is the process duration, $Y_{p,out}$ is the recovery yield defined as the ratio of the amount of mass recovered in the fraction collected in the outlet to the amount contained in the feed:

$$Y_{p,out} = \frac{m_{product}}{V_{inj}\, c_{p,F}} \tag{16}$$

To optimize the performance for given feed concentration the following problem can be solved:

$$Pr_p(\boldsymbol{x}) \Rightarrow \max \tag{17}$$

where $\boldsymbol{x}$ is a vector of decision variables, i.e., the operating parameters, which can be manipulated to alter the process productivity.

Optimization of the multiple-injection technique can involve several decision variables such as: variables determining the injection profile of the protein: $c_{p,F}$, t_{inj}, t_{wash}, (Eq. (11)), as well as of salt $c_{salt,F}$, $c_{salt,wash}$ (Eq. (12)) and the shape of the salt gradient, $c_{salt,j}$, Δt_j (Eq. (13)). Additionally, temperature and pH profile can be optimized.

The process productivity is maximized subject to constraints regarding the purity of the target product in the fraction collected:

$$\mathrm{Pu}_p \ \geq \ \mathrm{Pu}_{p,\min} \tag{18}$$

Pu_p is defined as follows:

$$\mathrm{Pu}_p = \frac{\bar{c}_{p,out}}{\sum_k^{NC} \bar{c}_{k,out}} \tag{19}$$

where $\bar{c}_{p,out}$ is the average concentration of the component p in the fraction collected, NC is the number of components k in the feed mixture. The purity constraints determine the cut time of the pure fractions.

If the protein solubility in the mobile phase is low the process performance can be limited by the solubility constraints. To prevent protein precipitation in the effluent stream the protein concentration at the column outlet can be constrained as follows:

$$c_{p,out} < \mathrm{sol} \tag{20}$$

Solubility, sol, can be a function of the salt concentration, temperature and pH of the mobile phase: sol = $f(c_{salt}, T, pH)$.

3. Experimental

3.1. Instruments and chemicals

3.1.1. Instruments

The HPLC instrument Äkta purifier with UV and conductometric detectors and a data station (GE Healthcare Life Sciences, Uppsala, Sweden) were used. The injector was a Rheodyne sampling valve with 100 μL and 500 μL sample loop.

Low temperature thermostat Lauda Re110 (Lauda, Lauda-Königshofen Germany) was used.

3.1.2. Materials and process conditions

In hydrophobic interaction chromatography as a stationary phase Butyl Sepharose 4FF (GE Healthcare Life Sciences) was used, in IEC cation exchanger UNOsphere S from Bio-Rad (Warsaw, Poland) was used (pore size 120 nm). The adsorbents were packed into the glass columns, length L = 12.5 cm, I.D. = 0.4 cm.

Three model proteins: cytochrome C (**Cyt**), Pu > 95%, pI = 10; ovalbumin (**Oval**), Pu > 98%, pI = 5; bovine immunoglobulin G (**IgG**), Pu > 95%, heterogeneous with pI > 5.6 were purchased from Sigma–Aldrich (Sigma–Aldrich, Poznan, Poland).

A 50 mM sodium phosphate buffer, pH = 7 was prepared as the elution buffer. The salt buffer (AS) was ammonium sulphate at concentration 1.7 M dissolved in phosphate buffer. Solutions pH were: pH = 7 for HIC, pH = 5–7 for IEC.

The mobile phase was a mixture of AS salt buffer and phosphate buffer with different volume ratios.

The mobile phase composition varied within the range 0–80% v/v (0–1.4 M) of AS salt buffer in isocratic experiments or 0–100% v/v (0–1.7 M) in the gradient elution.

Temperature investigated was: 5, 10, 15, 25 °C.

The mobile phase flowrate was 1.0 mL/min that correspond to the superficial velocity $u = 0.133$ m/s.

The proteins were dissolved to a concentration ca. 1 g/L or 0.5 g/L.

To measure the total bed porosity D-(+)-glucose (Sigma–Aldrich) was used. For HIC the value $\varepsilon_t = 0.95$ was found (the same packed bed was used as in our previous study [16]), for IEC the value $\varepsilon_t = 0.99$ was determined.

3.2. Procedures

3.2.1. Isocratic elution

For isocratic experiments similar procedure was used to that described in our previous studies [16]. Briefly, the samples of proteins were dissolved in the mobile phase and eluted in isocratic mode at different salt content in the mobile phase and at different temperature.

The protein profiles registered by the detector (at 280 nm wavelength) were converted into the concentration units by the calibration factors. For the detector calibration the same sample of each protein was injected into the system twice: into the column and directly into the detector bypassing the column. The calibration factor, cal, was calculated by integration of the UV profile of the protein bypassing the column (bypass peak) registered at the flowrate $\dot{V}$:

$$\mathrm{cal} = \frac{c_F V_{inj}}{\dot{V} \int \mathrm{UV}dt} \tag{21}$$

Then, the calibration factor was used to convert the protein profile at the column outlet (column peak) to concentration units. In such a way the mass losses of protein eluting from the column could be observed directly by comparing the integrals in Eq. (21) for the bypass and the column peak.

In HIC process mass losses were observed for **Oval** and **IgG**. For **Cyt** no mass losses in eluting peaks were observed regardless the process conditions.

In IEC elution similar effect of mass losses was observed depending on the salt concentration and pH. For **Oval** mass losses were small – ca. 15% at pH = 5 regardless the salt concentration; the effect vanished with increase of pH and for pH ≥ 6 was negligible. For **IgG** significant mass loses were observed at very low AS salt concentration in the mobile phase (0–0.12 M) at pH 5. The phenomenon diminished with increase of pH. For **Cyt** no mass losses were observed.

3.2.2. Elution in the sample-solvent

To analyze the effect of the sample-solvent on the chromatographic elution the proteins were dissolved in phosphate buffer free of AS salt and eluted with the mobile phase in the isocratic mode. If the band splitting occurred a part of protein co-eluted with phosphate buffer; hence, the detector signal of the protein and the sample-solvent were superimposed [16]. In this case to calibrate the detector signal the proteins dissolved in the sample-solvent were injected twice: into the column and into the bypass. Additionally, a blank pulse of the sample-solvent without protein was injected twice in the same way. For both elution lines (through the column and through the bypass) the detector signal of the blank pulse was subtracted from the peak of protein. The calibration coefficient was determined for the bypass peak after subtraction of the blank pulse (see details in [16]).

3.2.3. Gradient experiments

The step gradient was performed by switching the flow of the mobile phase from the column to the bypass (to fill the extra-column volumes with a new solution) or vice versa.

For the detector calibration each gradient elution of protein was followed by elution of the blank impulse of the sample-solvent with the same gradient program. Then, the elution of protein and the blank pulse was performed through the bypass. To convert the detector signal into the concentration profile analogous procedure was used as described above.

3.2.4. Band profiles of salt

To register and analyze the band profiles of salt in the multiple-injections and in the gradient elution the conductometric detector was additionally used. The calibration of the detector signal was performed for different salt concentration. A calibration curve was used to convert the detector signal to the concentration units.

3.2.5. Solubility measurements

Solubility of **IgG** in aqueous solution was significantly lower than that of the remaining model proteins, therefore, it constituted the performance constraint. Solubility of **IgG** was measured at different AS salt concentration, pH and temperature. For the measurement an excess of the solid sample of the protein was mixed with solutions containing different salt concentration. The closed tubes with the solutions were placed into the water bath in glass vessels equipped with the water jacket. Temperature in the water bath was controlled by a thermocouple. The tubes were left at given temperature (5, 15 or 25 °C) for 24 h; the saturated solutions were mixed with magnetic stirrers. Next, the samples of solutions were taken for the analysis to the Äcta systems, i.e., samples were injected into the detector bypassing the column. The injections of samples were followed by injections of blank pulses of the sample-solvents. The concentration of **IgG** in the saturated solutions was calculated after peak correction and integration.

3.2.6. Determining the model parameters

To predict chromatographic elution several model parameters have to be determined such as the equilibrium constant, K_p, the desorption rate coefficient, $k_{d,p}$, the dispersion coefficient, D_L, and the parameters quantifying folding–unfolding process: K_{unf}, k_f Eqs. (1, 2 and 4)).

The product of the external porosity and the axial dispersion coefficient ($\varepsilon_e D_L$) was evaluated as follows (see the form of Eq. (1)):

$$\varepsilon_e D_L = \frac{\varepsilon_e L w}{N_e} = \frac{L w}{N} \tag{22}$$

where L is the column length, $w = u/\varepsilon_t$, is the interstitial velocity, N_e is the number of theoretical plates, $N = N_e/\varepsilon_e$ is the apparent number of theoretical plates corresponding to the dispersion effects.

The apparent plate number, N, was determined for each system component, i.e., for proteins and salt, from width at half peak height of unretained (or very weakly retained) band profiles registered at buffer free of AS salt as the mobile phase. For unretained peaks the contribution of kinetic effects to band broadening could be neglected. The following values were obtained:

for HIC: $N_{\mathbf{IgG}} = 7.5$, $N_{\mathbf{Oval}} = 11.2$, $N_{\mathbf{Cyt}} = 14.6$, $N_{salt} = N_{H+} = 15.0$,
for IEC: $N_{\mathbf{IgG}} = 6$, $N_{\mathbf{Oval}} = 11.5$, $N_{\mathbf{Cyt}} = 12.2$, $N_{salt} = N_{H+} = 14.1$.

The column efficiency reported above corresponded to relatively high superficial velocity ($u = 0.133$ m/s); it increased markedly with the flowrate reduction for the proteins being investigated as well as for the salt ions (see Eq. (22)). Note that the dispersion coefficient, D_L is also a function of the mobile phase

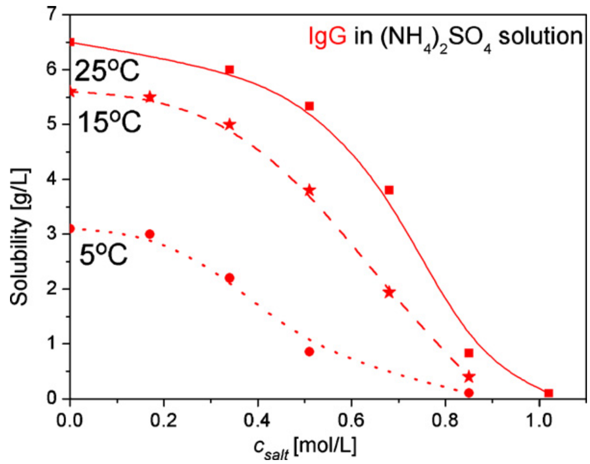

Fig. 1. Solubility of **IgG** in $(NH_4)_2SO_4$ solution.

velocity. However, in this study the effect of the flowrate on the process performance was not investigated.

Such a procedure for evaluation of $\varepsilon_e D_L$ was found to be more adequate than the use of empirical correlations; the dispersion coefficient evaluated by the Gunn equation [25] was found to be underestimated.

The values of $\varepsilon_e D_L$, were set constant for each component, i.e., independent of the process conditions. The remaining parameters, i.e., K and k_d, for cases when no conformational changes were detected (no mass losses) or K, k_d, K_{unf}, k_f, for cases of the protein unfolding, were determined by peak fitting (see details in [16]). A set of parameters was obtained for different salt concentration and temperature for HIC process and for different salt concentration and pH for IEC. Next, proper functional dependencies were determined (see details for the procedure in [16]):

- in HIC process four dependencies for **IgG** and **Oval** were determined: K_p, $k_{d,p}$, K_{unf}, $k_{unf}=f(c_{salt}, T)$, for **Cyt** only two, i.e,: K_p, $k_{d,p}=f(c_{salt}, T)$. Because no conformational changes were detected for **Cyt** the coefficients K_{unf}, k_{unf} were set equal to zero,
- in IEC process four functional dependencies were determined: K_p, $k_{d,p}$, K_{unf}, $k_{unf}=f(c_{salt}, \mathrm{pH})$ for **IgG** and **Oval**, while for **Cyt** only two parameters: K_p, $k_{d,p}=f(c_{salt}, \mathrm{pH})$.

Several dependencies had to be determined for each component, which required huge experimental efforts. Because of that the number of experimental measurements in isocratic mode (salt concentration, temperature and pH) was reduced to a minimum necessary to reproduce only general trends of parameter changes. Nevertheless, the quality of simulations with the model incorporating these dependencies was found to be satisfactory (see below, Section 4.3).

Ions constituting AS salt and hydrogen ions were unretained under the process conditions, i.e, the partition coefficient was set equal to zero $K_{salt}=0$, while $k_{d,salt}$ value was set sufficiently high to neglect the contribution of kinetic effects. The non-idealities of the system were accounted for by the dispersion coefficient D_L, determined based on the salt peak shape as described above.

4. Results and discussion

4.1. Solubility of IgG

The solubility measurements were performed according to the procedure described in Section 3.2.4. The results of measurements depicted in Fig. 1 indicate increase of solubility with increasing temperature and decreasing AS salt buffer concentration. The plateau of the solubility dependence within the range 0–0.17 M of AS salt might indicate a slight maximum between these values related to the optimal sample-solvent composition. However, the course of the curve and the retention data acquired on the HIC media suggest only a very minor solubility change within this concentration range. Therefore, buffer free of AS salt was used as the optimal sample-solvent.

The solubility was found to be practically independent of pH for pH = 5–7 (the results of measurements vs. pH are not depicted here). The reason of this phenomenon might be heterogeneity of **IgG** that had no unique isoelectric point. The results of measurements were used to quantify a functional dependence: $\mathrm{sol}=f(c_{salt}, T)$.

4.2. Retention behavior under isocratic conditions

To quantify retention pattern and kinetic coefficients isocratic experiments were performed for both HIC and IEC column under different operating conditions. In HIC process the salt concentration and temperature were used as the process variables; in IEC elution the salt concentration and pH were altered.

To simplify the experimental procedure and the mathematical description of the process kinetics and thermodynamics the same salt type (i.e., ammonium sulphate, AS) was used to alter the retention properties in both IEC and HIC system. In case of HIC the presence of AS salt enhanced retention, while in IEC reduced it. Note that the integration of both chromatographic techniques involves transferring the mobile phases between the systems during the injection period. Therefore, the presence of different types of ions would require determining complex multidimensional retention dependencies. Nevertheless, the extension of the concept of the injection technique for different salt systems is straightforward.

Illustration of retention behavior in HIC process is presented in Fig. 2. It can be observed that the protein adsorption represented by k' (retention factor) and the phenomenon of protein unfolding represented by K_{unf} (unfolding equilibrium constant) enhanced with increase of temperature and salt concentration with agreement to trends reported in literature [16,18,26].

IgG was found to be the most strongly adsorbed protein and most susceptible to the conformational changes.

The trends observed for the remaining parameters were similar to that analyzed in our previous study [16]. Therefore, for the sake of brevity, in Fig. 2 only the most representative results of measurements were shown.

Cyt under conditions investigated in HIC was very weakly retained regardless the salt concentration and temperature; model coefficients for this protein, K_p and $k_{d,p}$ were evaluated by peak fitting and averaged for all experiments.

The retention behavior of proteins in IEC is presented in Fig. 3. The retention pattern was reversed compared to HIC; retention of protein decreased with increasing salt concentration (Fig. 3a–d). Adsorption was strongly affected by pH; at pH 5 strong adsorption of **IgG** and **Cyt** was observed (Fig. 3c). Adsorption of **IgG** occurred only within a narrow range of low salt concentrations. At pH > 6 only **Cyt** was strongly adsorbed (Fig. 3d), **IgG** was slightly adsorbed only in the absence of AS salt; the adsorption completely vanished at pH = 7, **Oval** was unretained at pH > 6.

The phenomenon of the mass losses was also observed in IEC elution. As mentioned in Section 3.2.1 **Oval** lost irreversibly ca. 15% of mass at pH = 5 regardless the salt concentration. It could be completely eluted only at pH ≥ 6. For **IgG** the phenomenon of the mass losses was very pronounced (see Fig. 3e). The mass losses of **IgG** in IEC process might originate from the lack of unique isoelectric point. However, because this phenomenon was also observed for different homogeneous proteins such as **Oval** and **BSA** (for **BSA**

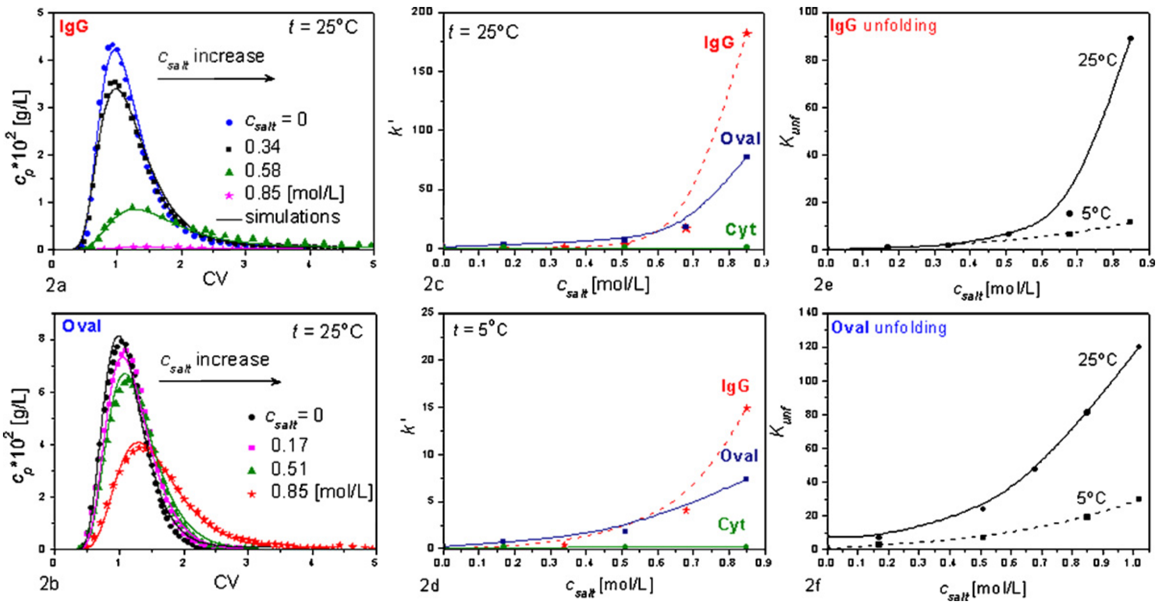

Fig. 2. Retention behavior in HIC process (a) and (b) typical changes of the band profiles for **IgG** and **Oval** vs. the salt concentration (c_F for **Oval** 1 g/L, for **IgG** 0.5 g/L); symbols – experimental data, lines simulations; (c) and (d) changes of the retention factor k' ($k' = FK_p$) vs. the salt concentration at 25 and 5 °C, (e) and (f) changes of K_{unf} vs. the salt concentration and temperature for **Oval** and **IgG**.

data not shown), the reason for such a behavior was attributed to the conformational changes of proteins. The possibility of conformational changes on ion exchange resins due to strong binding to active sites on the adsorbent surface has already been reported in literature [24,27,28]. Nevertheless, in this study this phenomenon has not been deeply investigated. Because the proteins being studied did not desorb in the unfolded state the presence of unfolded forms could not be detected by means of simple chromatographic experiments. For this purpose more sophisticated methods have to be used (see, e.g., [26]). As the conformational changes of IgG in the IEC system have been not proved the kinetic parameters concerning folding–unfolding process presented here should be considered as empirical parameters that allow the process prediction but whose physical sense needs to be verified.

4.3. Multiple-injection technique

As mentioned above to increase the loading concentration or avoid the operation of buffer exchange between chromatographic stages different solvents can be used to inject and elute the feed components. It has been shown that though this technique is useful for increasing the feed concentration, it restricts volumes of injections [16].

The origin of negative effects caused by increase of the injection volume is explained schematically in Fig. 4 on the basis of the equilibrium theory. The plot demonstrates hypothetical trajectory of a protein and a sample-solvent along the HIC column. The slope of the trajectory (characteristic line) is reversely proportional to the propagation velocity of the concentration fronts along the column.

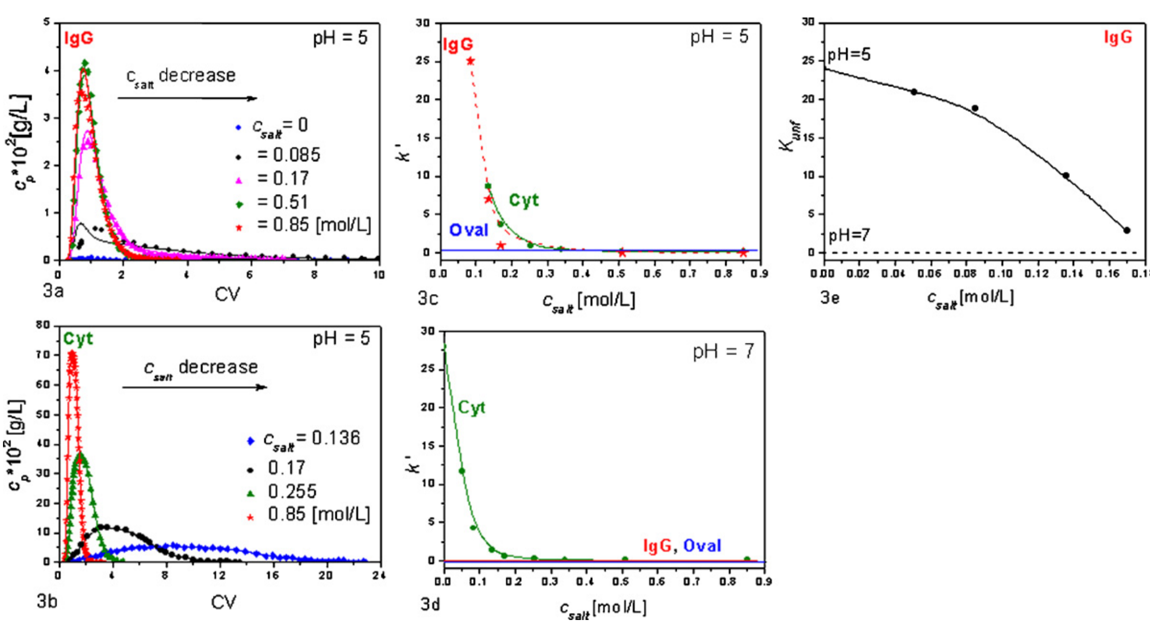

Fig. 3. Retention behavior in IEC process (a) and (b) typical changes of the band profiles for **IgG** and **Cyt** (c_F for **Cyt** 1 g/L, for **IgG** 0.5 g/L); symbols – experimental data, lines simulations; (c) and (d) changes of retention factor k' vs. the salt concentration at pH = 5 and 7, (e) changes of K_{unf} vs. the salt concentration and pH for **IgG**.

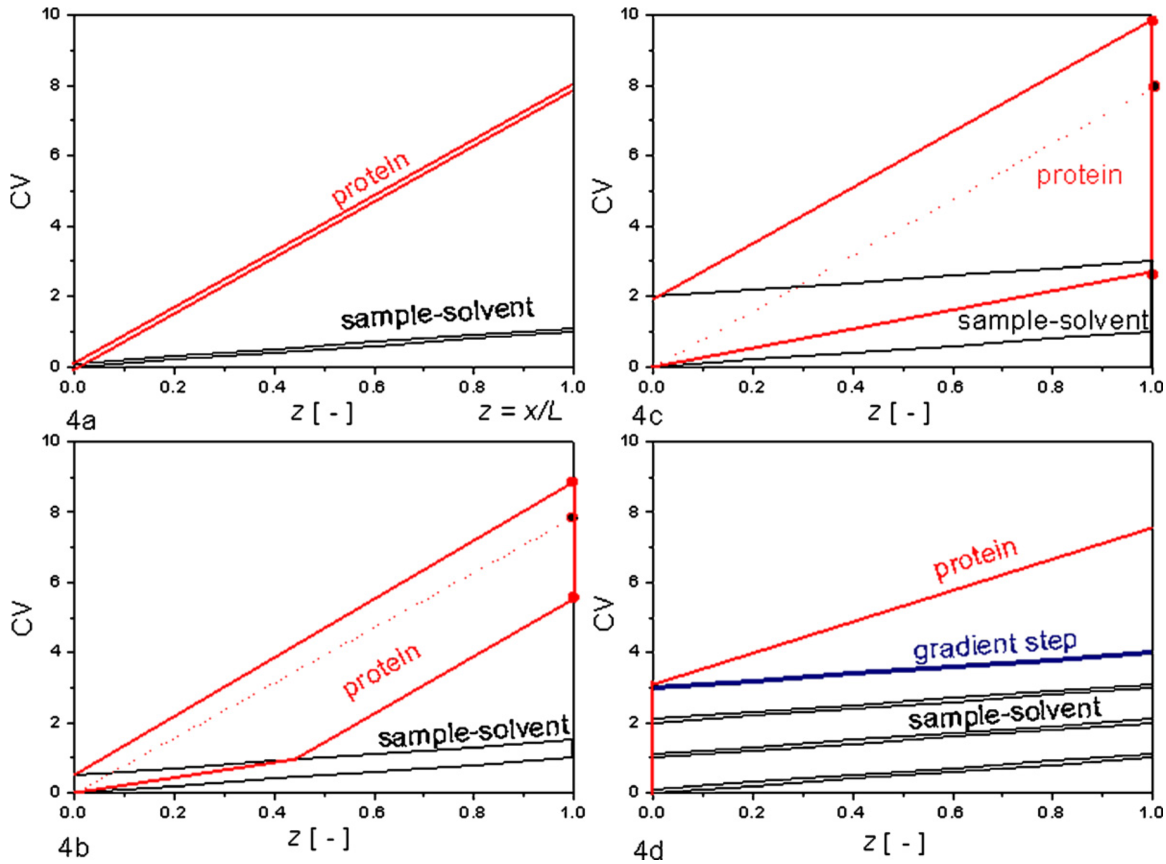

Fig. 4. Illustration of the sample-solvent effect vs. the injection volume under ideal conditions. Solid lines – trajectory of concentration fronts for the sample-solvent and protein. Dashed line – hypothetical trajectory of protein dissolved in the mobile phase.

For small-volume injections (Fig. 4a) the concentration fronts of protein and sample-solvent can travel independently along the column due to significant differences in their retention properties. Therefore, the bands of protein and sample-solvent can be easily separated at the column outlet. However, increase of the injection volume causes that the solute co-elutes with the sample-solvent (Fig. 4b). It results in a perturbation of the solute trajectory and band broadening. The phenomenon enhances with increase of the injection volume making chromatographic process inefficient (Fig. 4b and c).

To overcome such undesirable effects the multiple-injection technique can be employed. It is realized by several injections of small feed volumes under conditions of strong protein adsorption. Such injection conditions allow diminishing interactions between the sample-solvent and solute. The idea of this process is shown if Fig. 4d. The solute accumulates within the column during injections while the sample-solvent is unretained. Then, the solute separated from the sample-solvent can be eluted in a gradient mode.

Fig. 4 illustrates an ideal situation, for which all kinetic and dispersion effects are neglected. In a real column the band profiles of proteins as well as of the sample-solvent broaden due to kinetic and dispersion effects. However, the effect of the sample-solvent dilution facilitates realization of the multiple-injections.

To elucidate this phenomenon the propagation of the sample-solvent along the HIC column was demonstrated in Fig. 5, which illustrates elution of a pulse of buffer free of AS salt with the washing-solvent containing 1.7 M of AS salt. It can be observed that for a small injection volume the vacancy peak of AS salt dilutes

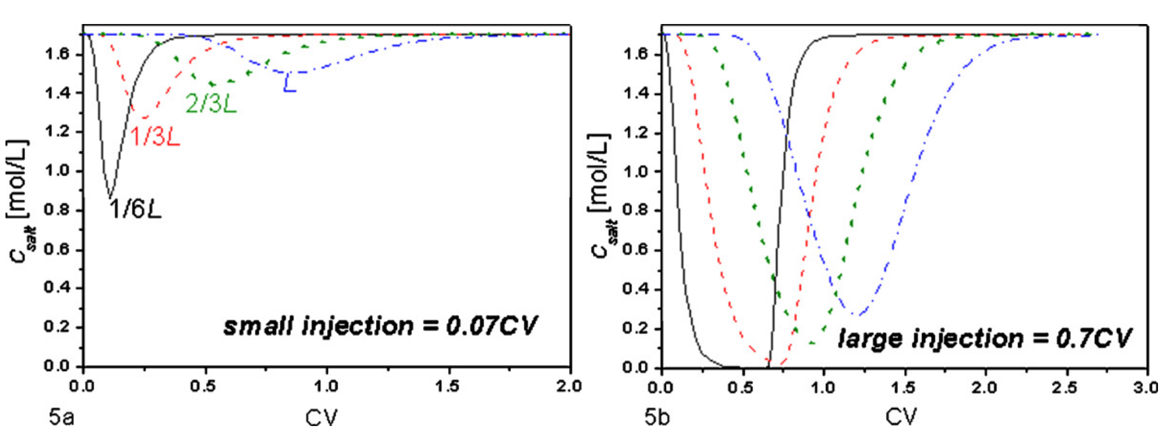

Fig. 5. Illustration of the vacancy peak dilution vs. the injection volume. Simulations by the dynamic model.

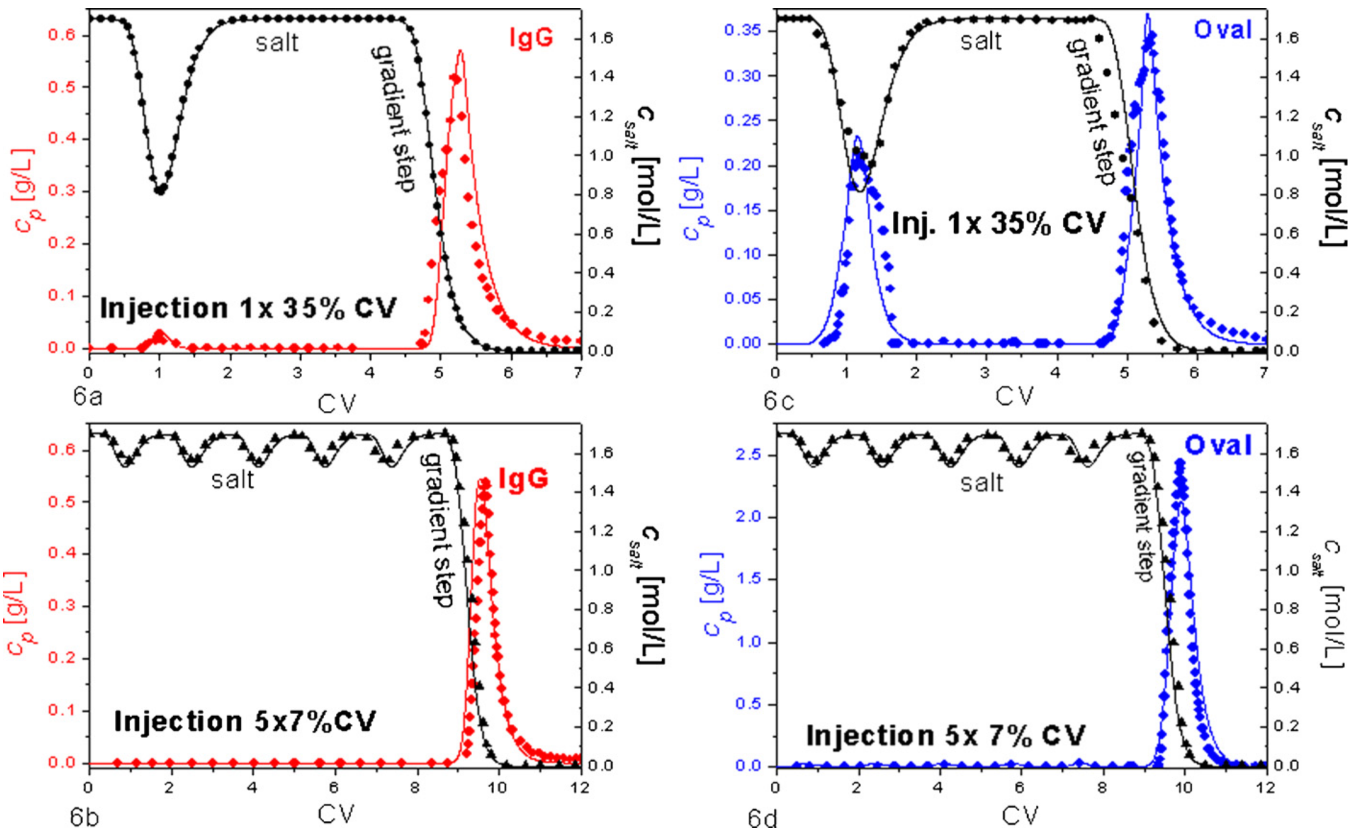

Fig. 6. Elution of **IgG** and **Oval** in the sample-solvent in HIC (a) and (c) large injection volume; (b) and (d) multiple-injection technique. Symbols – experimental data, lines simulations.

propagating along the column; the concentration in the peak minimum at the column outlet is only slightly lower than that in the washing-solvent (Fig. 5a). For large injections the minimum of the vacancy peak correspond to much lower AS concentration (Fig. 5b). For the latter case changes of retention properties of the protein which co-elutes with the sample-solvent might be significant.

This phenomenon can be exploited to realize the multiple-injections which are illustrated in Fig. 6. Fig. 6a and c demonstrate the column response to relatively large injection (500 μL ≅ 0.35CV) of **IgG** and **Oval**, respectively.

The proteins were dissolved in buffer free of AS salt and injected into the stream of highly concentrated salt solution (washing-solvent: 1.7 M AS salt). The injection cycle was followed by elution with a single gradient step (1.7–0 M AS salt). For large injection a part of protein was co-eluted with the vacancy peak. This was particularly visible for **Oval**, which was weaker adsorbed compared to **IgG** and could be easier eluted with the sample-solvent. Nevertheless, injecting the same mass but in few small-volume injections could prevent co-eluting the protein with the sample-solvent (Fig. 6b and d). For the latter case the concentration of AS salt in the vacancy peak was high enough to retain the protein inside the column under salting-out conditions.

Because **Cyt** was practically unretained it was co-eluted with the vacancy peaks of salt during multiple-injections (results not shown in Fig. 6). Therefore, HIC process enabled separation of **Cyt** from mixtures of **Oval** and **IgG**.

The same idea of the injection technique was successfully used in IEC despite the retention pattern of proteins was quite different than that observed in HIC. The proteins were dissolved in solutions of 0.085 M AS salt at pH = 7 and injected into the stream of buffer free of AS salt with pH 5 (washing-solvent). Proper adjusting of the injection volumes assured strong retention of **IgG** during the injection cycle and weak adsorption of **Oval**, which was co-eluted with the sample-solvent. The column response to the multiple-injections of **Oval** and **IgG** are illustrated in Fig. 7. Such a manner of elution allows separation and concentration of proteins in the effluent stream (see Fig. 7).

In IEC process **Cyt** was adsorbed simultaneously with **IgG** (results not shown in Fig. 7), therefore, only **Oval** could be separated from mixtures of **IgG** and **Cyt**.

4.4. Model simulations and optimization

To predict experimental profiles in chromatographic elution the dynamic model was used (Eqs. (1–14)). The model parameters and their functional dependencies on the salt concentration, temperature and pH were determined as described in Section 3.2.5 and incorporated into the model. The set of the model equations was solved for proteins, AS salt and hydrogen ions (pH profile) with proper boundary conditions. The temperature change was assumed to occur instantaneously. The model was solved by use of a finite difference method (see details elsewhere [22])

The results of simulations were compared to the experimental data (see Figs. 6 and 7); the model predictions were found to reproduce experiments with sufficient accuracy.

The model after verification was used to optimize the integrated process of HIC and IEC without desalting operation between the chromatographic steps. In this study a simple optimization procedure was exploited aimed to illustrate the integration strategy and possible benefits of the multiple-injection technique. The optimization routine was based on the modified Nelder–Mead algorithm [29]. Because the present study was not focused on this aspect, only a brief description of the optimization procedure is presented below.

Two combinations of the process integration were considered for separation of hypothetical ternary mixture **Cyt**, **IgG** and **Oval**

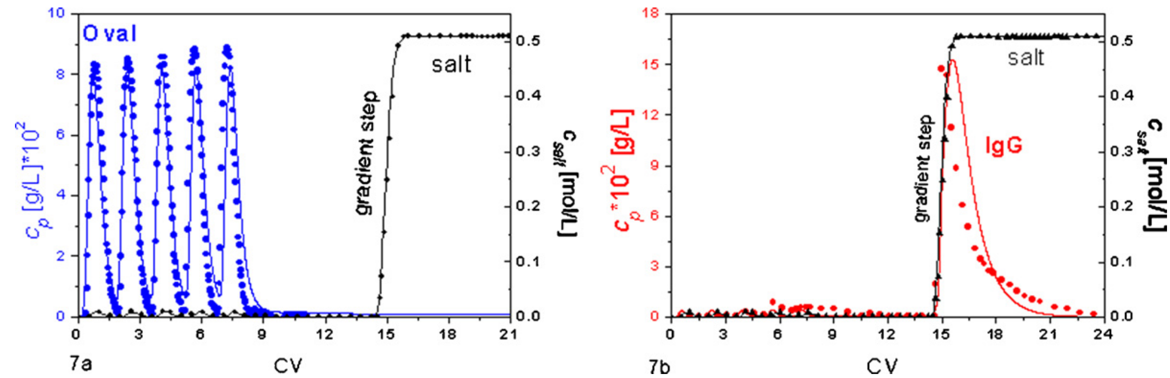

Fig. 7. Elution of **IgG** and **Oval** in the sample-solvent in IEC, multiple-injection technique: (a) **Oval**, (b) **IgG**. Symbols – experimental data, lines simulations.

with the feed concentration $c_F = 5$ g/L for each protein (1:1:1). The column dimensions and flowrate were set the same as used in experiments.

4.4.1. Combination I

*4.4.1.1. HIC as the first step designed to separate **Cyt** from the mixture of **Oval** and **IgG**.* In this step the proteins were assumed to be dissolved in buffer free of AS salt, injected into the column equilibrated with the washing-solvent containing 1.7 M AS salt and washed with the same solvent. The injection cycle was followed by two-step gradient consisting of "separation" and "desorption" step. The AS salt concentration in the desorption step, $c_{\text{salt},2}$, was set equal to 0 (buffer free of AS salt). The process temperature for all steps was set equal to 25 °C except temperature for the desorption step, which could be altered to facilitate desorption.

The following decision variables were optimized: injection time t_{inj}, washing time t_{wash}, (Eq. (11)), number of injection cycles n_{cyc}, the concentration of AS salt buffer and duration time for the first gradient step, i.e., $c_{\text{salt},1}$, Δt_1 (Eq. (13)) and temperature for the desorption step, T_2. The start of the fraction collection and the end of the process was determined by the threshold concentration of protein, $c_{\text{thresh}} < (c_{\text{F}}/1000)$.

The objective function was modified in the following way:

$$Pr_{\mathbf{IgG+Oval}} = \frac{V_{\text{inj}}(c_{\mathbf{IgG}}Y_{\mathbf{IgG},\text{out}} + c_{\mathbf{Oval},\text{F}}Y_{\mathbf{Oval},\text{out}})}{\Delta t_{\text{c}}} + \frac{V_{\text{inj}}c_{\mathbf{Cyt},\text{F}}Y_{\mathbf{Cyt},\text{out}}}{\Delta t_{\text{s}}} \tag{23}$$

where Δt_{c} corresponding to $\Delta\text{CV}_{\text{c}}$ is the collection time of the target fraction (see Fig. 8a), Δt_{s}, corresponding to $\Delta\text{CV}_{\text{s}}$, is the elution time of the rejected profile.

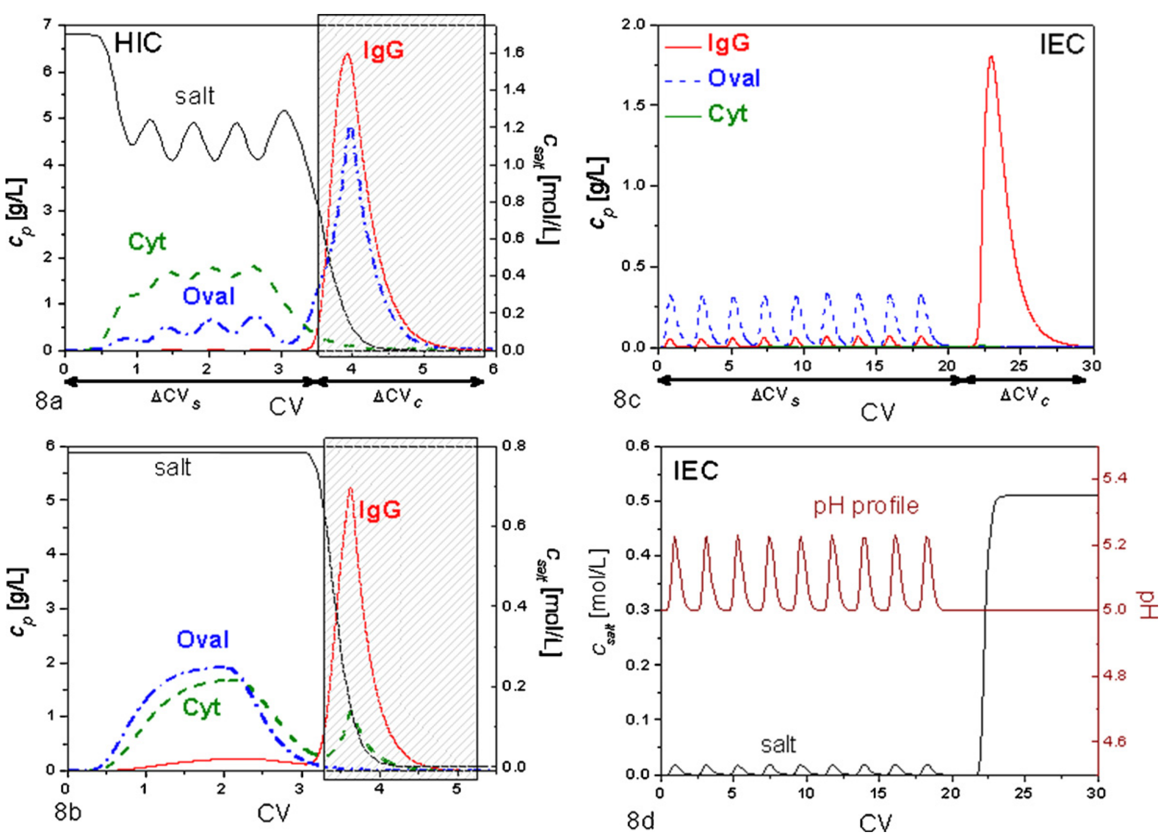

Fig. 8. Results of optimization for combination I. Optimal decision variables; (a) HIC as the first stage in the multi-injection mode, $c_{\text{salt1}} = 0.75$ M of AS salt, $t_{\text{inj}} = 19.1$ s, $t_{\text{wash}} = 37.1$ s, $t_{\text{grad1}} = 23.2$ s, $n_{\text{cycl}} = 4$; (b) HIC as the first stage in the isocratic injection mode, $c_{\text{salt}} = 0.78$ M of AS, $t_{\text{wash}} = 107.8$ s, $t_{\text{grad1}} = 0$; (c) IEC in the second stage $t_{\text{inj}} = 25.1$ s, $t_{\text{wash}} = 178.6$ s, $t_{\text{grad1}} = 0$; (d) corresponding salt and pH profiles for IEC stage. $\Delta\text{CV}_{\text{s,c}} = \Delta t_{\text{s,c}}/t_0$ (see Eq. (23), t_0 – inert retention).

Table 1
Performance indicators for the optimized separation process of the model proteins.

	$PR_P = \dot{m}_P$ (g/s) (Eq. (15))	$Y_{\mathbf{IgG}} = m_{\mathbf{IgG}}/m_{inj}$ (Eq. (16))
Single stage: HIC isocratic injection, P = **IgG** + **Oval**	1.02×10^{-5}	0.66
Single stage: HIC multiple-injection, P = **IgG** + **Oval**	7.17×10^{-6}	0.89
Two-stage, HIC first, P = **IgG**	1.58×10^{-6}	0.88
Two stage, IEC first, P = **IgG**	3.7×10^{-6}	0.88

Such a modification allowed reduction of fractionation time (i.e., the volume of the recycled fraction) and the duration time of the overall process.

The objective function was optimized subject to two constrains:

(1) purity constraints (see Eqs. (18 and 19)): Pu 97%

Pu was defined as follows:

$$Pu_{\mathbf{IgG}+\mathbf{Oval}} = \frac{\bar{c}_{\mathbf{IgG},out} + \bar{c}_{\mathbf{Oval},out}}{\bar{c}_{\mathbf{IgG},out} + \bar{c}_{\mathbf{Oval},out} + \bar{c}_{\mathbf{Cyt},out}} \tag{24}$$

(2) constraints of **IgG** solubility (see Eq. (20)): $c_{\mathbf{IgG},out} < sol(c_{salt,out}, T)$.

The results of optimization are presented in Fig. 8a and Table 1.

To demonstrate the advantages of the multiple-injection technique suggested the same separation process was optimized basing on traditional technique of isocratic injection. The same mass was assumed to be injected as that eluted in the multiple-injections. The pulse of single injection was followed by the salt gradient. A two-step salt gradient was initially assumed for the protein elution, however, optimization results indicated that the single-step gradient comprising only the desorption step, i.e., $t_{grad1} = 0$, performed better. Two decision variables were used in the optimization procedure, i.e., $c_{salt,1}$ and t_{wash}. The sample was assumed to be dissolved and injected in the mobile phase with the optimized salt concentration, $c_{salt,}$, that restricted the sample concentration, c_F, according to the solubility limits, and in turn, forced the values of the injection time, $t_{inj,}$ necessary to inject the assumed mass of the sample. The chromatogram corresponding to the optimal condition is presented in Fig. 8b. The comparison of the performance indicators for the separation process exploiting the multi- and isocratic injections is presented in Table 1. It can be observed that the injection time of feed mixtures can be shorter for the isocratic injections compared to that for multi-injections, which, for the former case, improves the process productivity. However, the productivity increase comes at the expense of yield that is very poor. For the isocratic injection mode an improvement of yield from 66% reported in Table 1 to ca. 75% requires much higher salt concentration in the mobile phase compared to the multiple-injection technique, which results in drastic reduction of the feed concentration (due to the solubility limits), increase of the elution time and significant peak dilution. As a consequence the process productivity drops by almost one order magnitude compared to the multi-injection technique.

*4.4.1.2. IEC as the second step designed to separate **Oval** from **IgG**.* The fraction of **Oval** and **IgG** collected in the effluent of HIC column was assumed to be recycled into the IEC process. Hence, the inlet concentrations in the IEC process were set equal to the average concentration of the proteins and salt in the recycled fraction. The washing-solvent was buffer free of AS salt with pH 5, which assured strong adsorption of **IgG**. Also in this case the single-step gradient, i.e., $t_{grad1} = 0$, was found to perform better than the two-step elution. The AS salt concentration for the desorption step, $c_{salt,2}$, was set 0.68 M AS, arbitrarily. It was minimal salt concentration for which rapid desorption of proteins was observed during experimental investigations.

Total volume of injections was set equal to the volume of the fraction withdrawn in the HIC step, which restricted the number of injection cycles, n_{cyc}. Temperature $t = 25\,^{\circ}C$ was set for the whole process. Eventually, two decision variables were used in the optimization procedure, i.e., t_{inj} and t_{wash}.

The goal function was defined as:

$$Pr_{\mathbf{IgG}} = \frac{V_{inj} c_{\mathbf{IgG},F} Y_{\mathbf{IgG},out}}{\Delta t_c} + \frac{V_{inj}(c_{\mathbf{Oval},F} Y_{\mathbf{Oval},out})}{\Delta t_s} \tag{25}$$

(1) Pr was optimized subject to the constraints: the purity constraints:

$Pu_{\mathbf{IgG}}$ 97%

Pu_i was defined as follows:

$$Pu_{\mathbf{IgG}} = \frac{\bar{c}_{\mathbf{IgG},out}}{\bar{c}_{\mathbf{IgG},out} + \bar{c}_{\mathbf{Oval},out} + \bar{c}_{\mathbf{Cyt},out}} \tag{26}$$

(2) **IgG** solubility constraints (see Eq. (20)): $c_{\mathbf{IgG},out} < sol$

The chromatograms corresponding to the optimal conditions are reported in Fig. 8c, the performance indicators are presented in Table 1. Additionally, corresponding salt and pH profiles were depicted in Fig. 8d. It is evident that strong dilution of salt and pH

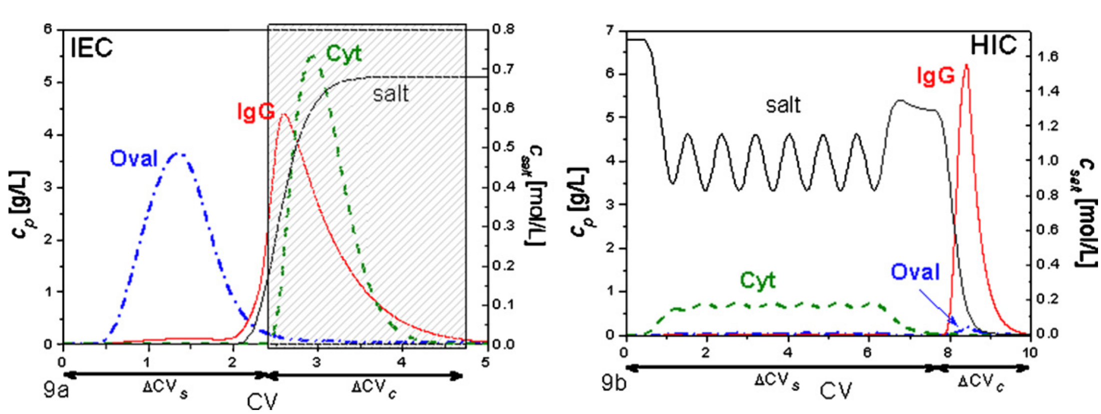

Fig. 9. Results of optimization for combination II. Optimal decision variables; (a) IEC in the first stage $t_{inj} = 233$ s, $t_{wash} = 103.8$ s, $t_{grad1} = 0$; (b) HIC in the second stage $c_{salt2} = 1.21$ M of AS salt, $t_{inj} = 33.8$ s, $t_{wash} = 38.7$ s, $t_{grad1} = 84.9$ s.

peaks enabled reducing interactions between the sample-solvent and proteins.

The isothermal conditions at $t = 25\,^\circ\mathrm{C}$ were found to be optimal for the overall process, which originated from the solubility constraints.

4.4.2. Combination II

*4.4.2.1. IEC as the first step designed to separate **Oval** from mixtures of **IgG** and **Cyt**.* Proteins were assumed to be dissolved and washed with the same solvent, i.e., buffer free of AS salt. Therefore, in this case the protein could be loaded in a single (large) injection. The proteins were eluted with a single desorption step as described above for combination I (IEC step).

The same mass of proteins was injected into the system as that in the combination I, which restricted the number of injection cycles. Therefore, two decision variables were optimized, i.e., t_{inj} and t_{wash}. The objective function was defined by:

$$Pr_{\mathbf{IgG+Cyt}} = \frac{V_{\mathrm{inj}}(c_{\mathbf{IgG}}\, Y_{\mathbf{IgG},\mathrm{out}} + c_{\mathbf{Cyt},\mathrm{F}}\, Y_{\mathbf{Cyt},\mathrm{out}})}{\Delta t_{\mathrm{c}}} + \frac{V_{inj}\, c_{\mathbf{Oval},\mathrm{F}}\, Y_{\mathbf{Oval},\mathrm{out}}}{\Delta t_{\mathrm{s}}} \tag{27}$$

The optimization was performed subject to the purity constraint, Pu 97%. Pu was defined as follows:

$$\mathrm{Pu}_{\mathbf{IgG+Cyt}} = \frac{\bar{c}_{\mathbf{IgG},\mathrm{out}} + \bar{c}_{\mathbf{Cyt},\mathrm{out}}}{\bar{c}_{\mathbf{IgG},\mathrm{out}} + \bar{c}_{\mathbf{Oval},\mathrm{out}} + \bar{c}_{\mathbf{Cyt},\mathrm{out}}} \tag{28}$$

and the solubility constraints as described above.

*4.4.2.2. HIC in the second step designed to separate **Cyt** from **IgG**.* The recycled form IEC fraction containing **Cyt** and **IgG** was assumed to be injected into the HIC column.

The following decision variables were optimized: t_{inj}, t_{wash}, $c_{\mathrm{salt},1}$, Δt_1 and temperature T_2 (see combination I, step HIC). The objective function was defined:

$$Pr_{\mathbf{IgG}} = \frac{V_{\mathrm{inj}} c_{\mathbf{IgG},\mathrm{F}} Y_{\mathbf{IgG},\mathrm{out}}}{\Delta t_{\mathrm{c}}} + \frac{V_{\mathrm{inj}} c_{\mathbf{Cyt},\mathrm{F}} Y_{\mathbf{Cyt},\mathrm{out}}}{\Delta t_{\mathrm{s}}} \tag{29}$$

the optimization was performed subject to the **IgG** purity using Eq. (26) and the solubility constraints.

The results of optimization are shown in Fig. 9a and b and Table 1.

The same mass of **IgG** with the same purity could be processed in both options of integrations, however combination II, i,e., IEC first, followed by HIC, could be realized faster due to possibility of feed loading in large single injection in the first separation stage. As it can be seen in Table 1, much higher productivity can be achieved for combination II at the same yield compared to combination I.

5. Conclusions

The multiple-injection technique was proposed to overcome efficiency limitation of the integrated chromatographic process for the protein separation such as the solubility constraint and to avoid the desalting operation between chromatographic stages. In this technique the proteins to be separated were dissolved in a sample-solvent and injected into the column by pulses with volumes sufficiently small to diminish negative effects of interactions with the sample-solvent during chromatographic elution.

The integration of two chromatographic stages based on HIC and IEC processes was considered. A dynamic model was used for the process design and optimization, which accounted for kinetic effects including those associated with conformational changes of proteins. The thermodynamic and kinetic coefficients were determined based on experiments of isocratic elution in HIC as well as in IEC column.

The experimental realization of the multiple-injection technique revealed improvement of the process performance compared to the standard isocratic injections in terms of concentration and volume of loadings.

The simulations performed indicated that the sequence of techniques in the integrated process can be optimized. The integrated process performed better if the technique involving the same solvent for the injection and elution was used in the first separation stage.

Acknowledgment

The financial support of Polish Scientific Committee within the grant no. N N209 004839 is greatly acknowledged.

References

[1] G. Carta, A. Jungbauer, Protein chromatography, in: Process Development and Scale Up, Wiley VCH, Weinheim, 2010.
[2] P. Kumpalume, S. Ghose, Chromatography: the high-resolution technique for protein separation, in: R. Hutti-Kaul, B. Mattiasson (Eds.), Isolation and Purification of Proteins, Marcel Dekker INC, NY, 2003.
[3] A.M. Azevedo, P.A.J. Rosa, I.F. Ferreira, M.R. Aires-Barros, J. Chromatogr. A 1213 (2008) 154.
[4] T. Fornstedt, G. Guiochon, Anal. Chem. 66 (1994) 2686.
[5] S. Golshan-Shirazi, G. Guiochon, Anal. Chem. 62 (1990) 923.
[6] S. Golshan-Shirazi, G. Guiochon, Anal. Chem. 61 (1989) 2373.
[7] W. Feng, X. Zhu, L. Zhang, X. Geng, J. Chromatogr. A. 729 (1996) 43.
[8] K.J. Williams, A. Li Wan Po, W.J. Irwin, J. Chromatogr. A. 194 (1980) 217.
[9] D. Vukmanic, M. Chiba, J. Chromatogr. 483 (1989) 189.
[10] P. Jandera, G. Guiochon, J. Chromatogr. 588 (1991) 1.
[11] G. Ströhlein, M. Mazzotti, M. Morbidelli, Chem. Eng. Sci. 60 (2005) 1525.
[12] G. Ströhlein, M. Morbidelli, H.K. Rhee, M. Mazzotti, AIChE J. 52 (2006) 565.
[13] G. Ströhlein, L. Aumann, L. Melter, K. Buescher, B. Schenkel, M. Mazzotti, M. Morbidelli, J. Chromatogr. A 1117 (2006) 146.
[14] K. Gedicke, M. Tomusiak, D. Antos, A. Seidel-Morgenstern, J. Chromatogr. A 1092 (2005) 142.
[15] K. Gedicke, D. Antos, A. Seidel-Morgenstern, J. Chromatogr. A 1162 (2007) 62.
[16] R. Muca, W. Marek, W. Piątkowski, D. Antos, J. Chromatogr. A 1217 (2010) 2812.
[17] J.A. Queiroz, C.T. Tomaz, J.M.S. Cabral, J. Biotechnol. 87 (2001) 143.
[18] E. Haimer, A. Tscheliessnig, R. Hahn, A. Jungbauer, J. Chromatogr. A. 1139 (2007) 84.
[19] M.E. Lienqueo, A. Mahn, J.C. Salgado, J.A. Asenjo, J. Chromatogr. B. 849 (2007) 53.
[20] Z. El Rassi, J. Chromatogr. A 720 (1996) 93.
[21] R. Muca, W. Piątkowski, D. Antos, J. Chromatogr. A. 1216 (2009) 8712.
[22] R. Muca, W. Piątkowski, D. Antos, J. Chromatogr. A. 1216 (2009) 6716.
[23] B.C.S. To, A.M. Lenhoff, J. Chromatogr. A 1141 (2007) 191.
[24] A. Voitl, A. Butté, M. Morbidelli, J. Chromatogr. A. 1217 (2010) 5492.
[25] D. Gunn, Chem. Eng. Sci. 42 (1987) 363.
[26] R. Ueberbacher, E. Haimer, R. Hahn, A. Jungbauer, J. Chromatogr. A 1198–1199 (2008) 154.
[27] S.C. Goheen, B.M. Gibbins, J. Chromatogr. A 890 (2000) 73.
[28] V. Noinville, C. Vidal-Madjar, B. SCbille, J. Phys. Chem. 99 (1995) 1516.
[29] G. Ziomek, D. Antos, L. Tobiska, A. Seidel-Morgenstern, J. Chromatogr. A 1116 (2006) 179.